A MEAN FIELD ANALYSIS OF THE FLUID/SOLID PHASE TRANSITION

CHARLES RADIN AND LORENZO SADUN

Abstract. We study the fluid/solid phase transition via a mean field model. Our first result is the derivation of a variational characterization of the entropy density, compatible with the infinite volume limit. We then determine the optimizing particle distributions for small energy density and a range of particle density, though we can only prove they are local, not global, minima of the entropy density. With this assumption we then prove that the resulting entropy density must lose its analyticity in various regimes. In particular this implies the existence of a phase transition between distinct heterogeneous structures at low energy density, and a phase transition between these structured phases and the disordered phase at high energy density.

1. Introduction

We will adapt an old random graph model of Strauss [St] to provide a mean field model of the fluid/solid phase transition of equilibrium matter, in particular to model how high density can produce the internal (crystalline) structure of solids out of a homogeneous fluid. The energy ground state in the model exhibits a range of different structures as the particle density varies, and we use this feature to show (to second order of perturbation theory) that there is a (solid/solid) phase transition between the structures, near the energy ground state, as well as a (fluid/solid) transition between the structured phases and the high energy disordered phase. We are forced to use a mean field model as there is still no convincing model of the basic phenomenon of a distinct solid phase; see [A, Br, Uh, Si, AR1]. We emphasize that ours is a toy model, in which the energy is not based on the physics of any real material but only has vaguely appropriate features of repulsion and attraction.

The following is the usual route for understanding the thermodynamic phases of a noble gas such as argon, using classical statistical mechanics and a Lennard-Jones, rotation symmetric, 2-body interaction potential V, depending on separation r by $V(r) = c_1 r^{-12} - c_2 r^{-6}$, with $c_1, c_2 > 0$; see Figure 1. This phenomenological interaction contains the desired features that the (neutral) atoms repel strongly at small separation due to their electron clouds, and deform at intermediate separation, providing a weak attraction responsible for the 'molecular bonds' in the solid phase. The two basic phase transitions, the gas/liquid and fluid/solid, are drawn schematically in Figure 2; neither can be proven for this model, and indeed it has yet to be proven even that the energy ground state is crystalline. (The appropriate crystal has been proven to be the unique ground state in 1 dimension [GR] and to be a ground state in 2 dimensions [T].)

Date: February 27, 2013.

2010 *Mathematics Subject Classification.* 82B26, 05C35, 05C80.

Key words and phrases. graphon, phase transition, mean-field, random graph.

This work was partially supported by NSF grants DMS-1208941 and DMS-1101326.

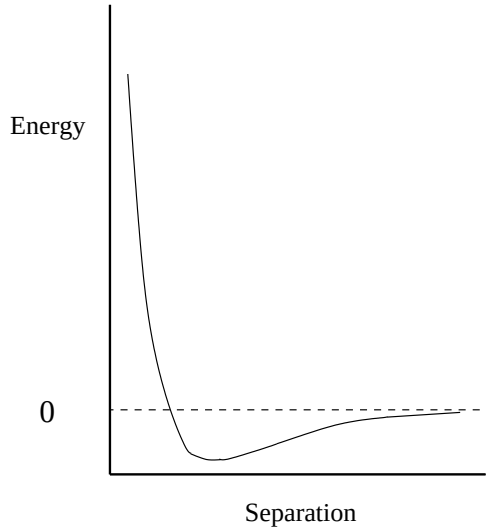

FIGURE 1. The Lennard-Jones interaction potential

Other, less-realistic models supply a convincing theoretical understanding for a gas/liquid transition for such materials. This was first achieved by the well known mean field model of van der Waals, in which the attraction between particles is simplified by ignoring the separation. See [LMP] for recent history of the model and improvements beyond mean field. These models reproduce the basic features of the transition as first order, with coexisting disordered phases of different energy and particle density, ending in a critical point; see Figure 2.

We note that not just for noble gases, but also for most materials, the gas/liquid transition is associated with an attractive force between the molecules. For argon the Lennard-Jones potential is reasonable, but for molecules which utilize other types of bonds in the solid phase a more complicated modeling would be desired. In contrast, the fluid/solid transition, at least at high pressure, is normally associated with the repulsion of the electron clouds of the molecules, independently of the detailed interaction associated with the outer electrons. The hard sphere model [Low], in which the only interaction is a simple hard core—two particles separated by less than the hard core distance produce infinite energy—is then appropriate quite generally, at least for roundish molecules. Simulation of the hard sphere model seems to show only a densely packed face centered cubic crystal ([BFMH, W]); the less-dense crystals which appear at lower pressure in some materials presumably are in part due to other features of the interaction, as in the simple cubic crystals of ionic solids such as table salt. Of course the hard sphere model does not show a gas/liquid transition since it does not include an attractive force. But the model does exhibit the basic phenomenon whereby (crystalline) structure is produced at high density.

Unfortunately our knowledge of the hard sphere model [Low], and more generally the theoretical understanding of the creation of crystalline structure at high density, is based almost completely on computer simulation [Br, Uh]. We will try to remedy this via an analogue of the van der Waals result, a mean field analysis but now for the fluid/solid transition. Following [PN, CD, AR1, AR2] we adapt a model of Strauss [St], with particles represented by edges in a large abstract graph and the (total) energy of a graph being the number of triangular subgraphs, providing a repulsion. Obviously this energy is not based

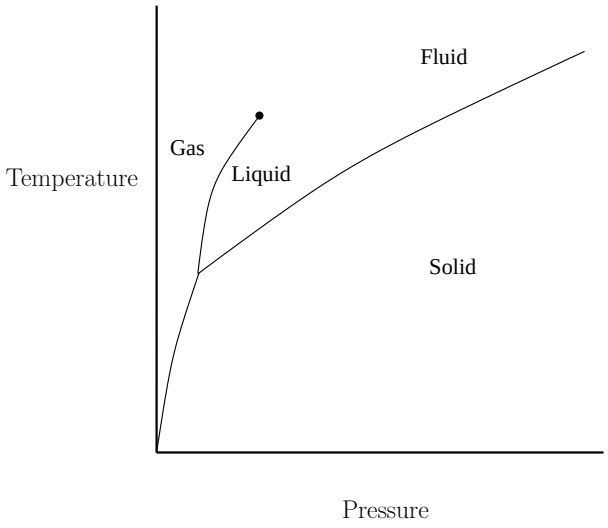

FIGURE 2. A schematic pressure/temperature phase diagram

on the physics of real interacting molecules. The features we use are the 'point' hard core, associated with the restriction that between given vertices no multiple edges are allowed, together with the soft repulsion associated with each triangle, a 3-body interaction. (As in the hard sphere model there is no attraction in our model; see however [PN, CD, RY] and references therein for a similar approach using attraction to model a gas/liquid transition.) Our argument depends on several recent results on the asymptotics of large graphs. We begin with notation; see [LS1, LS2, Lov, BCLSV, LS3, CD, CV] for background.

Consider the set $\hat{G}^n$ of simple graphs G with set $V(G)$ of (labelled) vertices, edge set $E(G)$ and triangle set $T(G)$, where the cardinality $|V(G)| = n$. ('Simple' means the edges are undirected and there are no multiple edges or loops.) Let $Z_{e,t}^{n,\delta}$ be the microcanonical partition function, the number of such graphs such that:

$$e(G) \equiv \frac{|E(G)|}{\binom{n}{2}} \in (e-\delta, e+\delta) \quad \text{and} \quad t(G) \equiv \frac{|T(G)|}{\binom{n}{3}} \in (t-\delta, t+\delta). \tag{1}$$

Graphs in $\cup_{n\geq 1}\hat{G}^n$ are known to have edge and triangle densities, (e,t), dense in the region R in the e,t-plane bounded by three curves, $c_1 : (e, e^{3/2})$, $0 \leq e \leq 1$, the line $l_1 : (e,0)$, $0 \leq e \leq 1/2$ and a certain scalloped curve $(e, f(e))$, $1/2 \leq e \leq 1$, lying above the curve $(e, e(2e-1))$, $1/2 \leq e \leq 1$, and meeting it when $e = e_k = k/(k+1)$, $k \geq 1$; see [PR] and references therein, and Figure 3.

We are interested in the relative density of graphs in R, more precisely in the entropy, the exponential rate of growth of the number of particle configurations (graphs) as n grows, as follows. First consider

$$s_{e,t}^{n,\delta} = \frac{\ln(Z_{e,t}^{n,\delta})}{n^2}, \text{ and } s_{e,t} = \lim_{\delta\to 0^+}\lim_{n\to\infty} s_{e,t}^{n,\delta}. \tag{2}$$

(The existence of the double limit will be proven.) We will measure the growth rate by the entropy density $s_{e,t}$, and the main question of interest for us is the existence of phase transitions (*i.e.* lack of analyticity of $s_{e,t}$) near the lower boundary of R in Figure 3. The

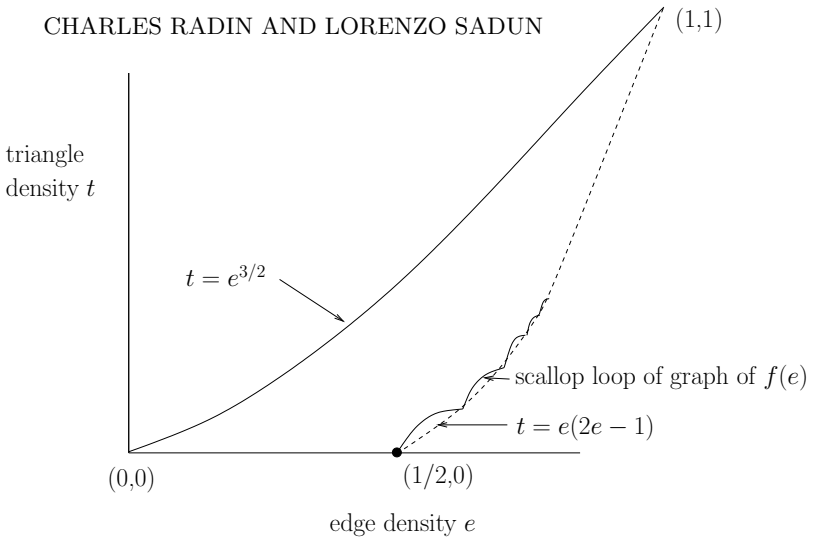

FIGURE 3. The microcanonical phase space R, outlined in solid lines

lower boundary consists of the scalloped curve together with the 'first scallop', the line from $(0,0)$ to $(1/2,0)$.

The analysis of phase transitions in traditional models with short range interactions requires the mathematical tools of the infinite volume limit. In this mean field graph setting appropriate tools have been developed recently under the title of 'graph limits', utilizing 'graphons', as we sketch next.

2. Graphons

Consider the set $\mathcal{W}$ of all symmetric, measurable functions

$$g : (x,y) \in [0,1]^2 \to g(x,y) \in [0,1]. \tag{3}$$

Think of each axis as a continuous set of vertices of a graph. For a graph $G \in \hat{G}^n$ one associates

$$g^G(x,y) = \begin{cases} 1 & \text{if } (\lceil nx \rceil, \lceil ny \rceil) \text{ is an edge of } G \\ 0 & \text{otherwise,} \end{cases} \tag{4}$$

where $\lceil y \rceil$ denotes the smallest integer greater than or equal to y. For $g \in \mathcal{W}$ and simple graph H we define

$$t(H,g) \equiv \int_{[0,1]^\ell} \prod_{(i,j)\in E(H)} g(x_i,x_j)\, dx_1 \cdots dx_\ell, \tag{5}$$

where $\ell = |V(H)|$, and note that for a graph G, $t(H,g^G)$ is the density of graph homomorphisms $H \to G$:

$$\frac{|\hom(H,G)|}{|V(G)|^{|V(H)|}}. \tag{6}$$

We define an equivalence relation on $\mathcal{W}$ as follows: $f \sim g$ if and only if $t(H,f) = t(H,g)$ for every simple graph H. Elements of $\mathcal{W}$ are called "graphons", elements of the quotient space

$\tilde{\mathcal{W}}$ are called "reduced graphons", and the class containing $g \in \mathcal{W}$ is denoted $\tilde{g}$. The space $\tilde{\mathcal{W}}$ is compact in the metric topology with metric:

$$\delta_{\blacksquare}(\tilde{f},\tilde{g}) \equiv \sum_{j\geq 1} \frac{1}{2^j} |t(H_j,f) - t(H_j,g)|, \tag{7}$$

where $\{H_j\}$ is a countable set of simple graphs, one from each graph-equivalence class. Equivalent functions in $\mathcal{W}$ differ by a change of variables in the following sense. Let Σ be the space of measure preserving bijections σ of $[0,1]$, and for f in $\mathcal{W}$ and $\sigma \in \Sigma$, let $f_\sigma(x,y) \equiv f(\sigma(x),\sigma(y))$. Then $f \sim g$ if and only if $g = f_\sigma$ for some $\sigma \in \Sigma$. Note that if each vertex of a finite graph is split into the same number of 'twins', each connected to the same vertices, the result stays in the same equivalence class, so for a convergent sequence $\tilde{g}^{G_j}$ one may assume $|V(G_j)| \to \infty$.

The value of this formalism here is that one can use large deviations on graphs with independent edges [CV] to give an optimization formula for $s_{e,t}$, which allows us to analyze $s_{e,t}$ near the energy ground states, the lower boundary of R in Figure 3. We next use the large deviations rate function for graphs with independent edges [CV] to give a variational characterization for the entropy density. (There is a variational characterization in [CD] of the analogous quantity for exponential random graph models.)

3. A variational characterization of the entropy density

Theorem 3.1. *For any possible pair (e,t), $s_{e,t} = -\min I(g)$, where the minimum is over all graphons g with $e(g) = e$ and $t(g) = t$, where*

$$e(g) = \int_0^1\int_0^1 g(x,y)\,dx\,dy, \qquad t(g) = \int_0^1\int_0^1\int_0^1 g(x,y)g(y,z)g(z,x)\,dx\,dy\,dz$$

and the rate function is

$$I(g) = \int_0^1\int_0^1 I_0(g(x,y))\,dx\,dy, \text{ where } I_0(u) = \frac{1}{2}\left[u\ln(u) + (1-u)\ln(1-u)\right]. \tag{8}$$

Proof. We first prove that $s_{e,t}$ is well-defined. A priori all we know is that $\liminf \ln(Z^{n,\delta}_{e,t})/n^2$ and $\limsup \ln(Z^{n,\delta}_{e,t})/n^2$ exist as $n \to \infty$. However, we will show that they both approach $-\min I(g)$ as $\delta \to 0^+$.

We need to define a few sets. Let U_δ be the set of graphons g with $e(g)$ and $t(g)$ strictly within δ of e and t, i.e. the preimage of an open square of side 2δ in (e,t)-space, and let F_δ be the preimage of the closed square. Let $\tilde{U}_\delta$ and $\tilde{F}_\delta$ be the corresponding sets in $\tilde{\mathcal{W}}$. Let $|U^n_\delta|$ and $|F^n_\delta|$ denote the number of graphs with n vertices whose checkerboard graphons (4) lie in U_δ or F_δ. The large deviation principle, Theorem 2.3 of [CV], implies that:

$$\limsup_{n\to\infty} \frac{\ln|F^n_\delta|}{n^2} \leq -\inf_{\tilde{g}\in\tilde{F}_\delta} I(\tilde{g}), \tag{9}$$

which also equals $-\inf_{g\in F_\delta} I(g)$, and that

$$\liminf_{n\to\infty} \frac{\ln|U^n_\delta|}{n^2} \geq -\inf_{\tilde{g}\in\tilde{U}_\delta} I(\tilde{g}), \tag{10}$$

which also equals $-\inf_{g\in U_\delta} I(g)$. This yields a chain of inequalities

$$-\inf_{U_\delta} I(g) \leq \liminf \frac{\ln|U_\delta^n|}{n^2} \leq \limsup \frac{\ln|U_\delta^n|}{n^2} \leq \limsup \frac{\ln|F_\delta^n|}{n^2} \leq -\inf_{F_\delta} I(g) \leq -\inf_{U_{\delta+\delta^2}} I(g) \tag{11}$$

As $\delta \to 0^+$, the limits of $-\inf_{U_\delta} I(g)$ and $-\inf_{U_{\delta+\delta^2}} I(g)$ are the same, and everything in between is trapped.

So far we have proven that

$$s_{e,t} = -\lim_{\delta\to 0^+} \inf_{U_\delta} I(g). \tag{12}$$

Next we must show that the right hand side is equal to $-\min_{F_0} I(g)$. By definition, we can find a sequence of reduced graphons $\tilde{g}_\delta \in \tilde{U}_\delta$ such that $\lim_{\delta\to 0} I(\tilde{g}_\delta) = \liminf_{U_\delta} I(g)$. Since $\tilde{W}$ is compact, these reduced graphons converge to a reduced graphon $\tilde{g}_0$, represented by a graphon $g_0 \in F_0$. Since I is lower-semicontinuous [CV], $I(g_0) \leq \lim I(g_\delta)$, so $\min_{F_0} I(g) \leq \liminf_{U_\delta} I(g)$. (We write min rather than inf since $\tilde{F}_0$ is compact.) However, $\min_{F_0} I(g)$ is at least as big as $\inf_{U_\delta} I(g)$, since $F_0 \subset U_\delta$. Thus $\min_{F_0} I(g) = \lim_{\delta\to 0} \inf_{U_\delta} I(g)$. □

4. Minimizing the rate function on the boundary

From now on we will work exclusively with graphons rather than with graphs. From Theorem 3.1, all questions boil down to "minimize the rate function over such-and-such region". The first region we study is the lower boundary of (e,t)-space, beginning with the first (flat) scallop:

Theorem 4.1. *If $e \leq 1/2$ and $t = 0$, then $\min_{F_0} I(g) = I_0(2e)/2$, and this minimum is achieved at the graphon*

$$g_0(x,y) = \begin{cases} 2e & \text{if } x < \frac{1}{2} < y \text{ or } y < \frac{1}{2} < x; \\ 0 & \text{otherwise.} \end{cases} \tag{13}$$

Furthermore, any other minimizer is equivalent to g_0, corresponding to the same reduced graphon.

Proof. Since $t(g)$ is identically zero, the measure of the set $\{(x,y) \in [0,1]^2 | g(x,y) = 0\}$ is at least $1/2$. Otherwise, the graphon $\bar{g}(x,y) = \begin{cases} 1 & \text{if } g(x,y) > 0; \\ 0 & \text{otherwise,} \end{cases}$ would have no triangles and would have edge density greater than $1/2$, which is impossible. So we restrict attention to graphons that are zero on a set of measure at least $1/2$. From the convexity of I_0, we know that the minimum of I among such graphons must be zero on a set of measure $1/2$ and must be constant on the rest . Thus g_0 is a minimizer, and $\min_{F_0} I(g) = I(g_0) = I_0(2e)/2$.

Now suppose that g is another minimizer. Since g is zero on a set of measure $1/2$ and is $2e$ on a set of measure $1/2$, $\bar{g}$ is 1 on a set of measure $1/2$, and so describes a graphon with edge density $1/2$ and no triangles. This means that $\bar{g}$ describes a complete bipartite graph with the two parts having the same measure. That is, $\bar{g}$ is equivalent to the graphon

that equals 1 if $x < \frac{1}{2} < y$ or $y < \frac{1}{2} < x$ and is zero everywhere else. But then $g = 2e\bar{g}$ is equivalent to g_0. □

The situation on the curved scallops is slightly more complicated. Pick an integer $\ell > 1$. (The case $\ell = 1$ just gives us our first scallop.) If $e \in \left[1 - \frac{1}{\ell}, 1 - \frac{1}{\ell+1}\right]$, then any graph G with edge density e and the minimum number of triangles has to take the following form (see [PR] for the history). Let

$$c = \frac{\ell + \sqrt{\ell(\ell - e(\ell+1))}}{\ell(\ell+1)}. \tag{14}$$

There is a partition of $\{1, \ldots, n\}$ into ℓ pieces, the first $\ell - 1$ of size $\lfloor cn \rfloor$ and the last of size between $\lfloor cn \rfloor$ and $2\lfloor cn \rfloor$, such that G is the complete ℓ-partite graph on these pieces, plus a number of additional edges within the last piece. ($\lfloor y \rfloor$ denotes the largest integer greater than or equal to y.) These additional edges can take any form, as long as there are no triangles within the last piece.

This means that, after possibly renumbering the vertices, the graphon for such a graph can be written as an uneven $\ell \times \ell$ checkerboard obtained from cutting the unit interval into pieces $V_k = [(k-1)c, kc]$ for $k < \ell$ and $V_\ell = [(\ell-1)c, 1]$, with the checkerboard being 1 outside the main diagonal, 0 on the main diagonal except the upper right corner, and corresponding to a zero-triangle graph in the upper right corner.

Limits of such graphons in the metric must take the form

$$g(x,y) = \begin{cases} 1 & x < kc < y \text{ or } y < kc < x \text{ for an integer } k < \ell; \\ 0 & (k-1)c < x, y < kc \text{ for some integer } k < \ell; \\ \text{unspecified} & x, y > (\ell-1)c, \end{cases} \tag{15}$$

with

$$\iiint\limits_{[(\ell-1)c,1]^3} g(x,y)g(y,z)g(z,x)\,dx\,dy\,dz = 0, \tag{16}$$

and with $\iint\limits_{[0,1]^2} g(x,y)\,dx\,dy = e$. Minimizing $I(g)$ on such graphons is easy, since all but the upper right corner of the graphon is fixed. Applying Theorem 4.1 to that corner, we get

Theorem 4.2. *If $e > 1/2$ and t is the smallest value possible, then the minimum of $I(g)$ on F_0 is achieved by the graphon*

$$g_0(x,y) = \begin{cases} 1 & x < kc < y \text{ or } y < kc < x \text{ for an integer } k < \ell; \\ p & (\ell-1)c < x < [1+(\ell-1)c]/2 < y \text{ or } (\ell-1)c < y < [1+(\ell-1)c]/2 < x; \\ 0 & \text{otherwise,} \end{cases} \tag{17}$$

where

$$p = \frac{4c(1-\ell c)}{(1-(\ell-1)c)^2} \tag{18}$$

is a number chosen to make $\iint_{[0,1]^2} g(x,y)\,dx\,dy = e$. *Furthermore, any other minimizer is equivalent to* g_0. *The minimum value of* $I(g)$ *is*

$$I(g_0) = \frac{(1-(\ell-1)c)^2}{2} I_0(p). \tag{19}$$

5. Minimizing near the first scallop

Now that we know the minimizer *at* the boundary, we perturb it to get a minimizer *near* the boundary.

Theorem 5.1. *Pick* $e < 1/2$ *and* ϵ *sufficiently small. Then the graphon*

$$g(x,y) = \begin{cases} 2e-\epsilon & x < \frac{1}{2} < y \text{ or } y < \frac{1}{2} < x \\ \epsilon & \text{otherwise,} \end{cases} \tag{20}$$

minimizes the rate function to second order in perturbation theory among graphons with $e(g) = e$ *and* $t(g) = e^3 - (e-\epsilon)^3$. *For pointwise small variations* δg *of* g, *the second variation in* $I(g)$ *is bounded from below by* $\frac{1}{2}\iint_{[0,1]^2} (\delta g(x,y))^2\,dx\,dy$.

Proof. We first consider the first variation in $I(g)$ for general graphons and derive the Euler-Lagrange equations. It is easy to check that our specific g satisfies these equations. We then consider the second variation in $I(g)$. Note that the function I_0 satisfies

$$I_0'(u) = \frac{1}{2}[\ln(u) - \ln(1-u)], \qquad I_0''(u) = \frac{1}{2}\left[\frac{1}{u} + \frac{1}{1-u}\right] \geq 2. \tag{21}$$

To find the Euler-Lagrange equations with the constraints that $(e(g), t(g))$ are equal to fixed values (e_0, t_0), we use Lagrange multipliers and vary the function $I(g) + \lambda_1(e(g)-e_0) + \lambda_2(t(g)-t_0)$. To first order, the variation with respect to g is

$$\delta I(g) = \int_0^1\int_0^1 I_0'(g(x,y))\delta g(x,y)\,dx\,dy + \lambda_1 \int_0^1\int_0^1 \delta g(x,y)\,dx\,dy \tag{22}$$

$$+3\lambda_2 \int_0^1\int_0^1 h(x,y)\delta g(x,y)\,dx\,dy, \tag{23}$$

where we have introduced the auxiliary function

$$h(x,y) = \int_0^1 g(x,z)g(y,z)\,dz. \tag{24}$$

Setting $\delta I(g)$ equal to zero, we get

$$I_0'(g(x,y)) = -\lambda_1 - 3\lambda_2 h(x,y). \tag{25}$$

Our particular $g(x,y)$ satisfies this equation with

$$3\lambda_2 = \frac{I_0'(2e-\epsilon) - I_0'(\epsilon)}{2(e-\epsilon)^2}. \tag{26}$$

Next we expand δt and δI to second order in δg, ignoring $O((\delta g)^3)$ terms.

$$\begin{aligned}
\delta I = \quad & \iint I_0'(g(x,y))\delta g(x,y)dx\,dy \\
& +\frac{1}{2}\iint I_0''(g(x,y))(\delta g(x,y))^2 dx\,dy \\
= \quad & \iint(-\lambda_1 - 3\lambda_2 h(x,y))\delta g(x,y)dx\,dy \\
& +\frac{1}{2}\iint I_0''(g(x,y))(\delta g(x,y))^2 dx\,dy \\
= \quad & -\lambda_1\delta e - \lambda_2\delta t + 3\lambda_2\iiint g(x,y)\delta g(x,z)\delta g(y,z)\,dx\,dy\,dz \\
& +\frac{1}{2}\iint I_0''(g(x,y))(\delta g(x,y))^2\,dx\,dy \\
= \quad & 3\lambda_2\iiint g(x,y)\delta g(x,z)\delta g(y,z)dx\,dy\,dz \\
& +\frac{1}{4}\iint I_0''(g(x,y))\delta g(x,y)^2 dx\,dy + \frac{1}{4}\iint I_0''(g(x,y))\delta g(x,y)^2 dx\,dy, \qquad (27)
\end{aligned}$$

since

$$\delta t = 3\iint h(x,y)\delta g(x,y)dx\,dy + 3\iiint g(x,y)\delta g(x,z)\delta g(y,z)dx\,dy\,dz + O((\delta g)^3), \qquad (28)$$

and since we are holding $e(g)$ and $t(g)$ fixed. We have split the $\iint I''\delta g^2$ term into two pieces, as we will be applying different estimates to each piece.

Since $h(x,y)$ and $I''(g)$ are piecewise constant, all of our integrals break down into integrals over different quadrants. Let R_1 and R_2 be the following subsets of $[0,1]^2$:

$$R_1 = \{x,y < 1/2\}\cup\{x,y > 1/2\}, \qquad R_2 = \{x < 1/2 < y\}\cup\{y < 1/2 < x\}. \qquad (29)$$

For each z, we define the functions $f_1(z) = \int_0^{1/2}\delta g(x,z)dx$ and $f_2(z) = \int_{1/2}^1 \delta g(x,z)dx$. The second variation in I is then

$$\begin{aligned}
& \frac{1}{4}\iint_{[0,1]^2} I_0''(g)\delta g(x,y)^2 dx\,dy + \frac{I_0''(\epsilon)}{4}\iint_{R_1}\delta g(x,y)^2 dx\,dy + \frac{I_0''(2e-\epsilon)}{4}\iint_{R_2}\delta g(x,y)^2 dx\,dy \\
+ \quad & 3\lambda_2\int_0^1 dz\left[\epsilon\iint_{R_1}\delta g(x,z)\delta g(y,z)dx\,dy + (2e-\epsilon)\iint_{R_2}\delta g(x,z)\delta g(y,z)dx\,dy\right] \\
= \quad & \frac{1}{4}\iint_{[0,1]^2} I_0''(g(x,y))\delta g(x,y)^2 dx\,dy + \frac{I_0''(\epsilon)}{4}\iint_{R_1}\delta g(x,z)^2 dx\,dz + \frac{I_0''(2e-\epsilon)}{4}\iint_{R_2}\delta g(x,z)^2 dx\,dz \\
& +3\lambda_2\int_0^1 \epsilon\left[f_1(z)^2 + f_2(z)^2\right] + 2(2e-\epsilon)f_1(z)f_2(z)\,dz \qquad (30)
\end{aligned}$$

Note that by Cauchy-Schwarz,

$$\int_0^{1/2} (\delta g(x,z))^2 dx \;\geq\; 2\left(\int_0^{1/2} \delta g(x,z) dx\right)^2 = 2f_1(z)^2 \tag{31}$$

$$\int_{1/2}^1 (\delta g(x,z))^2 dx \;\geq\; 2\left(\int_{1/2}^1 \delta g(x,z) dx\right)^2 = 2f_2(z)^2. \tag{32}$$

Since $I_0''(\epsilon)$ and $I_0''(2e-\epsilon)$ are positive, δI is bounded from below by

$$\begin{aligned} &\frac{1}{4}\iint\limits_{[0,1]^2} I_0''(g(x,y))\delta g(x,y)^2 dx\, dy + \frac{I''(\epsilon)}{2}\left[\int_0^{1/2} f_1(z)^2 dz + \int_{1/2}^1 f_2(z)^2 dz\right] \\ +\;& \frac{I_0''(2e-\epsilon)}{2}\left[\int_0^{1/2} f_2(z)^2 dz + \int_{1/2}^1 f_1(z)^2 dz\right] \\ +\;& 3\lambda_2 \int_0^1 dz\left[\epsilon(f_1(z)^2+f_2(z)^2) + 2(2e-\epsilon)f_1(z)f_2(z)\right] \end{aligned} \tag{33}$$

Collecting terms and applying equation (26), this bound becomes

$$\begin{aligned} \frac{1}{4}\iint\limits_{[0,1]^2} I_0''(g(x,y))\delta g(x,y)^2 dx\, dy \;+\;& \int_0^{1/2} dz[c_1 f_1(z)^2 + c_2 f_2(z)^2 + 2c_3 f_1(z)f_2(z)] \\ +\;& \int_{1/2}^1 dz[c_1 f_2(z)^2 + c_2 f_1(z)^2 + 2c_3 f_1(z)f_2(z)], \end{aligned} \tag{34}$$

where

$$c_1 \;=\; \frac{I_0''(\epsilon)}{2} + \frac{\epsilon(I_0'(2e-\epsilon) - I_0'(\epsilon))}{2(e-\epsilon)^2} \tag{35}$$

$$c_2 \;=\; \frac{I_0''(2e-\epsilon)}{2} + \frac{\epsilon(I_0'(2e-\epsilon) - I_0'(\epsilon))}{2(e-\epsilon)^2} \tag{36}$$

$$c_3 \;=\; \frac{(2e-\epsilon)(I_0'(2e-\epsilon) - I_0'(\epsilon))}{2(e-\epsilon)^2}. \tag{37}$$

Note that all coefficients are positive, and that $c_2 > 1$. As $\epsilon \to 0$, c_1 goes to $+\infty$ as $1/\epsilon$, while c_3 only diverges as $-\ln(\epsilon)$. Since $c_1 c_2 > c_3^2$ for small ϵ, the integrand for each z is positive semi-definite, so the integral over z is non-negative, and we obtain

$$\delta I \geq \frac{1}{4}\iint I_0''(g)\delta g^2 \geq \frac{1}{2}\iint \delta g(x,y)^2, \tag{38}$$

where we used the fact that $I_0''(u) \geq 2$ for all u. □

Any global minimizer must be $O(\epsilon)$ close to g_0, and hence $O(\epsilon)$ close to our specified perturbative minimizer. This means that the only way for them to differ is through a complicated bifurcation of minimizers at g_0, despite the uniform bounds on δI as we approach the boundary. The difference between these hypothetical minimizers and g_0 would not be pointwise small, but would merely be small in an L^1 sense.

For instance, consider graphons of the form

$$g(x,y) = \begin{cases} p & x < c < y \text{ or } y < c < x; \\ \alpha & x, y < c; \\ \beta & x, y > c, \end{cases} \tag{39}$$

where c is a parameter that we will vary and p, α and β are constants that depend on c. For each c sufficiently close to $1/2$, it is possible to find a graphon of this form such that $\iiint g(x,y)g(y,z)g(x,z)dx\,dy\,dz = t$ and $\iint g(x,y)dx\,dy = e$, and such that the Euler-Lagrange equations (25) are satisifed. Call this graphon $g_c(x,y)$. A lengthly calculation shows that

$$\left.\frac{\partial^2 I(g_c)}{\partial c^2}\right|_{c=1/2} \geq 16e^2 \tag{40}$$

for small t, indicating that (nearly) bipartite graphs with pieces of unequal size have a higher rate function than g. This provides strong evidence that our perturbative solution is in fact a global minimizer for sufficiently small t.

Corollary 5.2. *Assuming our perturbative solution is the global optimizer, there is a phase transition near the boundary point* $(1/2, 0)$ *between the first and second scallop.*

Proof. Our perturbative solution yields a formula for the entropy:

$$s_{e,t} = -\frac{1}{2}[I_0(\epsilon) + I_0(2e - \epsilon)]. \tag{41}$$

This formula for the entropy cannot be extended analytically beyond $e = (1+\epsilon)/2$, as $\partial^2 s/\partial e^2$ diverges as $e \to (1+\epsilon)/2$. However, $e = (1+\epsilon)/2$ corresponds to $t = (\epsilon^3 + 3\epsilon)/4$, or, using the more basic variable e,

$$t = [(2e-1)^3 + 3(2e-1)]/4, \tag{42}$$

which is in the interior of (e,t) space. (Since the graphon $g(x,y)$ is nowhere zero, it differs in form from the graphons describing graphs with minimal t.) Thus $s_{e,t}$ must fail to be analytic in some neighborhood of the first scallop. □

Of course there must also be a phase transition, presumably from this bipartite phase to a homogeneous phase, if one fixes e and raises t, which we see as follows.

Corollary 5.3. *Assuming our perturbative solution is the global optimizer, there is a phase transition as one raises* t*, for any fixed* $0 < e < 1/2$*.*

Proof. Recall from Corollary 5.2 the connection between t and ϵ:

$$t = \epsilon^3 - (e - \epsilon)^3. \tag{43}$$

Note that t is an increasing function of ϵ and reaches the value $2e^3$ when $\epsilon = 2e$. From equation (41) for the entropy we see that it cannot be extended analytically to $t > 2e^3$, yet for $e < 1/2$ we have $2e^3 < e^2 < e^{3/2}$ so (e,t) is in the interior of the phase space (Figure 3). □

6. Conclusion

Our goal is a theoretical understanding of why materials develop a solid phase at high enough particle density (pressure) and low enough energy density (temperature). As discussed in the introduction, this is presumably 'due to' the repulsive part of the intermolecular interaction. Simplifying the Lennard-Jones potential, the interaction $\tilde{V}(r) = r^{-12}$ for separation r should give the desired effect. Working in the microcanonical ensemble the main problem would be to show why, at high particle density, the energy ground state is crystalline and that this survives at low, not necessarily minimum, energy density. This has been a famous unsolved problem for many years [A, Br, Uh, Si, AR1].

We have taken an unusual path here in order to make some progress on this classic problem, working in a model in which there are energy ground states of different type as one varies the particle density. Such a model might have a phase diagram as in Figure 4. (A simple model using short range forces showing different crystal structures in the ground state in one spatial dimension is the 'shift model' [NR]. Of course the crystal structures do not survive to higher energy density in one dimensional models such as that.)

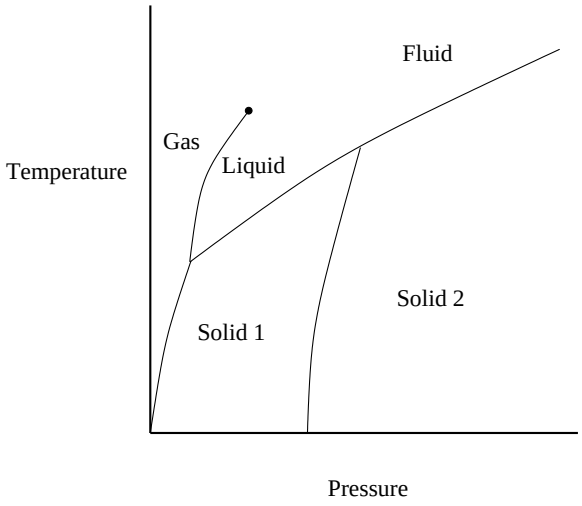

Figure 4. A schematic pressure/temperature phase diagram with different crystalline phases

Indeed, many real materials display a range of crystal structures. Most have a close packed crystal structure at high particle density, but many are looser packed at lower density, for instance simple cubic for table salt. This feature of varying crystal structure is useful for us because there is then a phase transition between the different crystal structures *near energy minimization*, the lower edge of the phase space in Figure 4. This is significant because one can use this to analyze the structure of the low energy phases, separately from analyzing whether those structured phases melt to a fluid.

This is the path we have taken in our mean field model. We have shown that our (2-parameter, bipartite) graphons g of Theorem 5.1 maximize the entropy density at least to second order in perturbation theory, among states with given, and low, particle and energy densities. Assuming the g are actually global maximizers we then proved the entropy density would have to lose analyticity as the density of the state approaches the tripartite regime. We also show that the entropy density must suffer a phase transition as the energy density

is raised sufficiently high, presumably from the structured bipartite phase to a homogeneous high energy phase.

We expect that a more complicated analysis could produce appropriate graphons $g^{(k)}$, $k \geq 1$, near each of the higher density (multipartite) ground states, with a transition near each scallop intersection. Intuitively this suggests a mechanism whereby as particle density is increased, near the energy ground state, the system progressively transitions through finer and finer structure; for high particle density most configurations would consist of many interacting 'parts', in a crude approximation to how the unit cells in a crystal behave.

Our results on phase transitions require that the graphons of Theorem 5.1 be in fact global, not just local, maximizers of the entropy density. In a future paper we use a symmetry to prove that these graphons are indeed the unique global maximizers at least for energy density in the range $0 \leq t \leq 1/8$ and particle density $e = 1/2$, and we can then see the transition on this curve. However we still cannot prove the graphons are the global optimizers of entropy density for (e, t) in a two-dimensional region, as is needed to fully justify the notion of a structured phase. (See [AR2] for a variant of this approach.)

In conclusion we emphasize that our key tool was Theorem 3.1, an optimization formula for the asymptotic entropy density, based on the graph limit formalism. The graphon formalism is a powerful tool for dealing with the infinite volume limit in mean field models, which we have used to make some small progress on the classic problem of the fluid/solid transition.

Acknowledgements: We gratefully acknowledge useful discussions with Francesco Maggi and Peter Winkler.

References

[A] P.W. Anderson, Basic Notions of Condensed Matter Physics, Benjamin/Cummings, Menlo Park, 1984, Chapter 2.

[AR1] D. Aristoff and C. Radin, Rigidity in solids, J. Stat. Phys. 144 (2011) 1247-1255.

[AR2] D. Aristoff and C. Radin, Emergent structures in large networks, J. Appl. Probab. (to appear), arXiv:1110.1912

[BCLSV] C. Borgs, J. Chayes, L. Lovász, V.T. Sós and K. Vesztergombi, Convergent graph sequences I: subgraph frequencies, metric properties, and testing, Adv. Math. 219 (2008) 1801-1851.

[BFMH] P.G. Bolhuis, D. Frenkel, S.-C. Muse and D.A. Huse, Nature (London) 388 (1997) 235-236 .

[Br] S. G. Brush, Statistical Physics and the Atomic Theory of Matter, from Boyle and Newton to Landau and Onsager, Princeton University Press, Princeton, 1983, 277.

[CD] S. Chatterjee, and P. Diaconis, Estimating and understanding exponential random graph models, arXiv: 1102.2650v3.

[CV] S. Chatterjee and S.R.S. Varadhan, The large deviation principle for the Erdös-Rényi random graph, Eur. J. Comb. 32 (2011) 1000-1017

[GR] C.S. Gardner and C. Radin, The infinite volume ground state of the Lennard-Jones potential J. Stat. Phys., 20 (1979), 719-724.

[LMP] J.L. Lebowitz, A.E. Mazel and E. Presutti, Liquid-vapor phase transitions for systems with finite-range interactions, J. Stat. Phys. 94 (1999) 955-1025.

[Lov] L. Lovász, Large networks and graph limits, American Mathematical Society, Providence, 2012.

[LS1] L. Lovász and B. Szegedy, Limits of dense graph sequences, J. Combin. Theory Ser. B 98 (2006) 933-957.

[LS2] L. Lovász and B. Szegedy, Szemerédi's lemma for the analyst, GAFA 17 (2007) 252-270.

[LS3] L. Lovász and B. Szegedy, Finitely forcible graphons, J. Combin. Theory Ser. B 101 (2011) 269-301.

[Low] H. Löwen, Fun with hard spheres, In: "Spatial Statistics and Statistical Physics", edited by K. Mecke and D. Stoyan, Springer Lecture Notes in Physics, volume 554, pages 295-331, Berlin, 2000.

[NR] F. Nicolò and C. Radin, A first-order phase transition between crystal phases in the shift model, J. Stat. Phys. 28 (1982) 473-478.

[PN] J. Park and M.E.J. Newman, Solution for the properties of a clustered network, Phys. Rev. E 72 (2005) 026136.

[PR] O. Pikhurko and A. Razborov, Asymptotic structure of graphs with the minimum number of triangles, arXiv:1203.4393

[RY] C. Radin and M. Yin, Phase transitions in exponential random graphs, Ann. Appl. Probab. (to appear), arXiv:1108.0649.

[Si] B. Simon, Fifteen problems in mathematical physics, in Perspectives in Mathematics: Anniversary of Oberwolfach 1984, Birkhäuser Verlag, Basil-Berlin-Boston, 1984, 442.

[St] D. Strauss, On a general class of models for interaction, SIAM Rev. 28 (1986) 513-527.

[T] F. Theil, A proof of crystallization in two dimensions, Comm. Math. Phys. 262 (2006), 209 - 236

[Uh] G.E. Uhlenbeck, in Fundamental Problems in Statistical Mechanics II, edited by E. G. D. Cohen, Wiley, New York, 1968, 16-17.

[W] L.V. Woodcock, Nature (London) 385 (1997) 141-143.

Charles Radin, Department of Mathematics, The University of Texas at Austin, Austin, TX 78712

E-mail address: radin@math.utexas.edu

Lorenzo Sadun, Department of Mathematics, The University of Texas at Austin, Austin, TX 78712

E-mail address: sadun@math.utexas.edu